eNeuro

Research Article: New Research | Sensory and Motor Systems

DREADD-induced silencing of the medial olfactory tubercle disrupts the preference of female mice for opposite-sex chemosignals

The mOT mediates females' pheromone preference

Brett T. DiBenedictis[a], Adaeze O. Olugbemi[a], Michael J. Baum[a] and James A. Cherry[b]

[1]*Department of Biology, Boston University, Boston, MA 02215, United States*
[2]*Department of Psychological and Brain Sciences, Boston University, Boston, MA 02215, United States*

DOI: 10.1523/ENEURO.0078-15.2015

Received: 16 July 2015

Revised: 21 August 2015

Accepted: 29 August 2015

Published: 8 September 2015

Author Contributions: BD, MB, and JC designed research; BD and AO performed research; BD MB, and JC analyzed data; BD, MB, and JC wrote the paper.

Funding: NIH: DC008962.

Conflict of Interest: The authors report no conflict of interest.

Correspondence should be addressed to Corresponding author at: Department of Psychological and Brain Sciences, Boston University, Boston, MA 02215, United States. Tel.: +1 617 353 3254. *E-mail address*: jcherry@bu.edu (J.A. Cherry)

Cite as: eNeuro 2015; 10.1523/ENEURO.0078-15.2015

eNeuro

http://eneuro.msubmit.net

eN-NWR-0078-15R1

DREADD-induced silencing of the medial olfactory tubercle disrupts the preference of female mice for opposite-sex chemosignals

DREADD-induced silencing of the medial olfactory tubercle disrupts the preference of female mice for opposite-sex chemosignals

Abbreviated Title: The mOT mediates females' pheromone preference

Brett T. DiBenedictis[a], Adaeze O. Olugbemi[a], Michael J. Baum[a], James A. Cherry[b,*]

[a] Department of Biology, Boston University, Boston, MA 02215, United States

[b] Department of Psychological and Brain Sciences, Boston University, Boston, MA 02215, United States

BD, MB, and JC designed research; BD and AO performed research; BD MB, and JC analyzed data; BD, MB, and JC wrote the paper

[*] Corresponding author at: Department of Psychological and Brain Sciences, Boston University, Boston, MA 02215, United States.
Tel.: +1 617 353 3254.
E-mail address: jcherry@bu.edu (J.A. Cherry)

Number of figures: 8
Number of tables: 2
Number of Multimedia: 0

Number of words--
Abstract: 245 (limit: 250)
Significance Statement: 115 (limit: 120)
Introduction: 591 (limit: 750)
Discussion: 1473 (limit: 3000)

Acknowledgments: We thank Alexander Helfand for his assistance with the development of our terminal odor exposure box and pilot CTb injections.

Conflict of interest: The authors report no conflict of interest.

Funding sources: This work was supported by NIH grant DC008962 awarded to JAC.

Abstract:

Attraction to opposite-sex pheromones during rodent courtship involves a pathway that includes inputs to the medial amygdala (Me) from the main and accessory olfactory bulbs, and projections from the Me to nuclei in the medial hypothalamus that control reproduction. However, consideration of circuitry that attributes hedonic properties to opposite-sex odors has been lacking. The medial olfactory tubercle (mOT) has been implicated in the reinforcing effects of natural stimuli and drugs of abuse. We performed a tract-tracing study wherein estrous female mice that had received injections of the retrograde tracer, CTb, into the mOT were exposed to volatile odors from soiled bedding. Both the anterior Me and ventral tegmental area (VTA) sent direct projections to the mOT, of which a significant subset was selectively activated (expressed Fos protein) by testes-intact male (but not female) volatile odors from soiled bedding. Next, the inhibitory DREADD receptor, hM_4Di, was bilaterally expressed in the mOT of female mice. Urinary preferences were then assessed after i.p. injection of either saline or clozapine-N-oxide (CNO), which binds to the hM_4Di receptor to hyperpolarize infected neurons. After receiving CNO, estrous females lost their preference for male over female urinary odors, whereas the ability to discriminate these odors remained intact. Male odor preference returned after vehicle treatment in counterbalanced tests. There were no deficits in locomotor activity or preference for food odors when subjects received CNO injections prior to testing. The mOT appears to be a critical segment in the pheromone-reward pathway of female mice.

Keywords: DREADD, hM_4Di, olfactory tubercle, retrograde tract tracing

Significance Statement:

This work adds to a growing body of evidence that the medial olfactory tubercle (often thought of as solely an olfactory cortical structure) encodes natural, reinforcing hedonic behaviors. Females' innate preference for male urinary odors was abolished when the mOT was silenced using DREADD methodology, but persisted under control conditions wherein the mOT was not silenced. Importantly, this effect was not due to a deficit in olfactory processing (i.e. an inability to discriminate between male and female urinary odors). Moreover, the female mOT is selectively activated by male urinary odors, and this activation appears to be driven mainly by MeA and VTA efferents. The mOT is a key node in the pheromone-reward pathway in mice.

Introduction:

The processing of social chemosignals (or 'pheromones') in the rodent brain occurs via hardwired circuitry involving either or both the main and accessory olfactory systems. For example, Choi et al. (2005) describe a "reproductive pathway" that transmits stimuli detected by the vomeronasal organ (VNO) to the accessory olfactory bulbs (AOB), and from there, to the medial amygdala (Me), which receives input from both the AOB and the main olfactory bulb (MOB). In turn, several nuclei in the medial hypothalamus receive projections from the Me. This model, however, does not incorporate structures known to be critical for attributing rewarding properties to opposite-sex pheromones, including regions of the ventral striatum that are required for sexual attraction (DiBenedictis et al., 2014b; Agustin-Pavon et al., 2014; Novejarque et al., 2011).

The nucleus accumbens (Acb) plays an important role in the reinforcing effects of drugs of abuse as well as natural stimuli (Roberts et al., 1977, 1979; McGregor & Roberts, 1993; Baker et al., 1998; Liao et al., 2000; Rodd-Henricks et al., 2002; Ikemoto & Sharpe, 2001; Heinz et al., 2009; Koob & Volkow 2010; Cassataro et al., 2014; Wang et al., 2013). However, additional evidence also implicates the medial olfactory tubercle (mOT) in both drug-induced as well as natural reinforcement (FitzGerald et al., 2014; Ikemoto 2003; Ikemoto et al., 2005). The mOT is a trilaminar structure that includes the cell bridges of the ventral pallidum (VP), the islands of Calleja (ICj), as well as a striatal component, consisting mainly of GABAergic medium spiny neurons (Ikemoto, 2010). Furthermore, the mOT receives direct input from the main olfactory bulb and recent evidence suggests that the mOT is an important center for encoding odor valence (White, 1965; Schwob and Price, 1984a; Wesson and Wilson 2011; Gadziola et al., 2015). Tract-tracing studies in female mice have shown that the mOT receives dense monosynaptic input from the Me (DiBenedictis et al., 2014a; Pardo-Bellver et al., 2012), and other results suggest that the preference of female mice to investigate opposite-sex chemosignals may involve the mOT (Agustin-Pavon et al., 2014). In that study, the medioventral striatopallidum (mvStP), a region including but not limited to the mOT, was damaged with electrolytic lesions that may have destroyed fibers of passage and also, in some cases, included adjacent brain regions. Moreover, it is unclear from that study whether the deficit in preference for male bedding odors reflects a hedonic/motivational defect or an inability to discriminate male vs female odorants. This distinction is especially important since the mvStP contains portions of the olfactory tubercle, a cortical olfactory structure. Finally, it remains to be seen whether male bedding

preference deficits persist when females have access to only the volatile components of the stimulus, activating only the main olfactory system. A strong demonstration that the mOT participates in processing attractive chemosignals would involve showing that the mOT receives inputs from the "reproductive pathway" that are selectively activated by opposite-sex odors in addition to demonstrating that selective inactivation of mOT neurons eliminates attraction to opposite-sex chemosignals. We addressed these issues in two experiments. First, we used tract-tracing in combination with male urinary odor-induced Fos co-expression to identify forebrain regions in female mice that innervate the mOT and are selectively activated by opposite-sex odors. Next, we used the pharmacosynthetic 'DREADD' (designer receptors exclusively activated by designer drugs) approach to reversibly silence mOT neurons in female mice (Armbruster et al., 2007; Rogan and Roth, 2011; Farrell and Roth, 2013). Our data suggest that activity in mOT neurons plays an essential role in motivating estrous female mice to seek out male pheromones.

Materials and Methods:

Subjects

Seventy-four female and 12 male Swiss Webster mice were purchased (Charles River Laboratories, Wilmington, MA, USA) at 5-6 weeks of age and housed in same sex groups under a reversed 12h light:dark cycle. At Charles River Laboratories, the pregnant Swiss-Webster female is removed from the male's cage and placed in a maternity cage well before parturition. Thus, the female offspring used in the present study did not have mating experience with a male, nor had they direct nasal access to

breeding male odors prior to arriving at Boston University. Females in the functional tract tracing study (Experiment 1) were housed 4 per cage for the duration of the experiment, while females in the DREADD study (Experiment 2) were housed 4 per cage until 48 hours prior to the start of behavioral testing, whereupon they were housed individually. All behavioral testing was video recorded and conducted under red light during the dark phase of the photoperiod. Food and water were provided *ad libitum*, except where otherwise noted. The Boston University Institutional Animal Care and Use Committee approved all procedures used in this study. Three days after arrival, female subjects as well as female bedding/urine donors underwent bilateral ovariectomy and were allowed 1 week to recover. Animals were implanted s.c. at the back of the neck with an estradiol (E_2) capsule at the time of ovariectomy (bedding/urine donors & Experiment 1 subjects) or at the time of DREADD virus or Vehicle infection surgery (Experiment 2 subjects).

Reagents

For all surgeries, subjects were anesthetized with 2% isoflurane vapor and were administered carprofen (5 mg/kg, s.c.) analgesic daily for two days after surgery. Estradiol was administered in polymeric silicone SILASTIC capsules (inner diameter, 1.57 mm; outer diameter, 2.41 mm; length, 5 mm) diluted 1:1 with cholesterol. Progesterone (P; 500 µg, s.c.) was injected 4 h prior to testing or urine collection to induce full behavioral estrus (E_2+P). The retrograde tracer, Cholera Toxin B (CTb, List Biological Laboratories, Campbell, CA) was used at 0.5% in 0.1 M phosphate buffer, pH 6.0. In the DREADD experiment, an adeno-associated virus containing the Cre

recombinase-independent viral construct, AAV5-hSyn-HA-hM$_4$D(Gi)-IRES-mCitrine (University of North Carolina Vector Core), was used to express the hM$_4$Di receptor and the fluorescent reporter mCitrine in neurons. When bound to the non-endogenous ligand, clozapine-N-oxide (CNO), hM$_4$Di induces somatic hyperpolarization and markedly reduces presynaptic neurotransmitter release (Armbruster et al., 2007; Ferguson et al., 2011; Rogan and Roth, 2011; Stachniak et al., 2014). Where used, CNO (Enzo Life Sciences, Farmingdale, NY) was administered i.p. in saline vehicle at 5 mg/kg 30 min prior to testing. This dosage and time of administration have been used previously to activate DREADD receptors (Sasaki et al., 2011; Farrell et al., 2012; Garner et al., 2012; Penagarikano et al., 2015). Immunolabeling procedures utilized primary antibodies for Fos, CTb, NeuN and green fluorescent protein (GFP; used to visualize mCitrine$^+$ neurons) (obtained from Santa Cruz Biotechnologies, Dallas, TX, List Biological Laboratories, EMD Millipore, Billerica, MA and MBL International, Woburn, MA, respectively), with secondary antibodies that included biotinylated donkey anti-rabbit (for Fos, Jackson ImmunoResearch Laboratories), biotinylated donkey anti-goat (for CTb, Jackson ImmunoResearch Laboratories), biotinylated horse anti-mouse/rabbit (for NeuN, Vector Laboratories, Burlingame, CA) and Alexa Fluor 488 donkey anti-goat (for GFP, Life Technologies, Carlsbad, CA). ABC reagents, diaminobenzidine (DAB) and VectaShield mounting medium with 4',6-diamidino-2-phenylindole (DAPI) were obtained from Vector Laboratories (Burlingame, CA).

Urine and soiled bedding collection

Urine used for odor preference, odor discrimination, and terminal odor exposure was collected from group housed, testes-intact male (n=12) and E_2-implanted ovariectomized female (n=12) donor mice using metabolic cages. Pooled urine was aliquoted into 1-ml vials according to sex and stored at -20°C until use. The same donor mice were placed in a cage with clean Aspen chip bedding for 24 hr. The soiled bedding was then collected and stored according to sex at -20°C until used as an olfactory stimulus for terminal odor exposures. Female bedding donors were first brought into estrus with a P injection 4 h before placing in the cage.

Stereotaxic Injections

Seven days following bilateral ovariectomy, mice were anesthetized and the head was secured in a stereotaxic apparatus (David Kopf Instruments, Tujunga, CA, USA. Small holes were then drilled bilaterally over each injection site (coordinates: anterior-posterior: 5.3 mm from interaural line, medial-lateral: 0.7 mm from sagittal suture, depth: 4.7 mm from dura). For retrograde tracer injections (Experiment 1), a glass micropipette (30-µm tip diameter) containing CTb was lowered into the rostral mOT and deposited iontophoretically by passing a pulsatile (7 s on 7 s off) cathodal current (+5 µA) for 5-8 min using a current source (Stoelting, Wood Dale, IL, USA). The pipette was left in place for 5 min post injection and withdrawn from the brain under a -5 µA anodal current to prevent backflow. For Experiment 2, 0.2-0.3 µl of either the virus ('hM_4Di') or sterile PBS ('Vehicle') was pressure injected at 0.25-0.3 µl/min using a 5-µl syringe with a 30-gauge needle (Hamilton Company, Reno, NV, USA) at the stereotaxic coordinates given above. The needle tip was left in place for 5-9 min before retracting. After injection, drill holes were filled with bone wax and incisions were closed with suture.

194

195 *Behavioral tests*

196 Locomotor Activity. Subjects were given an injection of CNO or saline 30 min before
197 placing individually in Plexiglas boxes (57 × 14 × 19 cm) inside an isolation cubicle (61
198 × 65 × 51 cm). Subjects' movements in the open field were tracked for the next 20 min
199 using a digital video camera and Any-Maze software (Stoelting Co., Wood Dale, Il,
200 USA). Subjects received two tests, one with and one without CNO, in counterbalanced
201 order separated by 2 days. Subjects did not receive P prior to these tests. Mean distance
202 traveled by subjects in each group was compared using a 2-way repeated measures
203 ANOVA, with Infection Type (hM_4Di vs Vehicle) and Drug Treatment (CNO vs Saline)
204 as factors.

205

206 Urinary Odor Preference. Two days following locomotor testing subjects received a non-
207 contact, *Volatiles Only* odor preference test for testes-intact male vs estrous female urine.
208 Testing took place in the homecage wherein subjects were simultaneously presented for 5
209 min with the two odors (20 µl each absorbed onto filter paper) placed 7 cm apart. To
210 restrict access to volatiles only, a wire mesh was placed over the odor source such that
211 direct nasal contact was prevented. The location of urinary odors was switched for each
212 test to control for any side bias. This test was administered twice (separated by 4 days),
213 in the presence or absence of CNO in counterbalanced order. As in other studies (Keller
214 et al 2006; Martel and Baum, 2009b; Brock et al, 2011) subjects previously implanted
215 with E_2 capsules were brought into estrus with an injection of P 4 h prior to each odor
216 preference test. These combined hormone treatments when given to ovariectomized

females induce all aspects of feminine courtship behavior, including lordosis and the motivation to seek out male chemosignals.

Four days later, preferences for urinary odors when nasal contact was permitted were assessed. Procedures followed for these *Volatiles+Nonvolatiles* tests were identical to the *Volatiles Only* tests except that the wire mesh barrier was removed allowing direct nasal access to the urine. Again, two tests were given at 4-day intervals using a counterbalanced (± CNO) design with P administered 4 h prior to testing. The *Volatiles Only* test was used to assess the specific contribution of the MOS, while the *Volatiles+Nonvolatiles* test assessed the contribution of both the MOS and AOS in pheromone processing.

Time spent actively investigating (defined as having the snout raised and oriented toward and within 1 cm of the stimulus) each odor during the 5 min test was recorded. Two-way repeated measures ANOVAs (followed by Student-Newman-Keuls *post hoc* tests, where applicable) were then used to assess effects of Infection Type and Drug Treatment on difference scores (time spent investigating intact male urine minus time spent investigating estrous female urine) for *Volatiles Only* and *Volatiles+Nonvolatiles* tests as well as on total investigation times (time spent investigating intact male urine plus time spent investigating estrous female urine) for each test.

Odor Discrimination. To verify that subjects could discriminate between testes-intact and estrous female urinary volatiles, subjects underwent a home-cage habituation/dishabituation test. Subjects did not receive P prior to these tests, since it has been previously shown in mice that both ovary-intact females (Isles et al., 2002) and

ovariectomized females given E_2 only (Martel & Baum 2009b; DiBenedictis et al., 2014b) can reliably discriminate between male and female urinary odors, as indexed by robust habituation/dishabituation responses to each urinary odor. Briefly, subjects were given three presentations of water followed by three presentations of estrous female urinary odor followed by three presentations of testes-intact male urinary odor. Physical access to urine was prevented using a wire mesh barrier. Subjects received two tests (separated by 2 days) in the presence or absence of CNO using a counterbalanced design. Paired *t*-tests were used to compare the mean investigation times for the dishabituation responses of each group: the third presentation of water vs the first estrous female urinary odor, as well as the third presentation of estrous female urinary odor vs the first presentation of testes-intact male urinary odor. The dishabituation responses were compared between groups using a 2-way repeated measures ANOVA with Infection Type and Drug Treatment as factors.

Cookie Odor Preference. Food was removed and subjects were given 2.5 g of Nutter Butter™ cookie. After two hours, residual cookie crumbs were removed from the cage and subjects were food-deprived for 24 h. A 5-min odor preference test was then administered in a format identical to the *Volatiles Only* odor preference test, except that the odors used were 20 µl cookie dissolved in mineral oil vs mineral oil alone. Subjects received two tests (separated by 2 days) in the presence or absence of CNO in counterbalanced order. Odor locations were switched for each test to prevent side bias. Subjects did not receive P prior to this test. The mean times spent investigating each

stimulus (cookie vs mineral oil) were calculated for each group and compared using paired *t*-tests.

Terminal Odor Exposure

Subjects were habituated in an odor exposure cage (28 × 16.5 × 12.7 cm) for 4 h in a dark fume hood. Because stress has been shown to induce Fos expression in many forebrain regions (including hypothalamic and amygdaloid nuclei; Cullinan et al., 1995), we used a setup in which subjects are not handled by the experimenter at the onset of odor exposure. This setup consisted of an exposure cage with a perforated floor that could be stacked on a second cage containing bedding that could not be physically contacted. To optimize females' physiological responses to biological odors, experiment 1 subjects were given an injection of P and placed in an exposure cage that was stacked on a cage with clean bedding. After 4 h, the exposure cage was placed over a second cage containing either clean bedding or soiled bedding from testes-intact males or estrous females. Experiment 2 subjects were treated in the same manner, except these subjects were always exposed to testes-intact male soiled bedding following a 4 h habituation. To insure an adequate odor environment, the male-soiled and estrous female-soiled beddings were spiked with 1 ml of male or estrous female urine, respectively, and cages were placed on a heating pad on low heat (~30°C) for the duration of exposure to maximize odor volatility.

Histological Analysis of CTb Uptake & hM_4Di Infection

For CTb and Fos double-labeling, tissues were first Fos-labeled, then re-fixed in 4% paraformaldehyde (PFA) for 10 min and washed in PBS before staining for CTb.

Briefly, 30-µm free-floating cryosections were incubated overnight in rabbit anti-c-Fos (1:1000) at RT followed by 1 h incubation with biotinylated donkey anti-rabbit secondary antibody. Sections were next incubated with ABC reagent and visualized using DAB with nickel enhancement. Sections were refixed for 10 min in 4% PFA before immunolabeling for CTb: goat anti-CTb primary antibody (1:40,000) followed by biotinylated donkey anti-goat secondary antibody, incubation with ABC reagent, and visualization using DAB without nickel enhancement. Thus, two different chromogens (DAB-nickel, black; and DAB-only, brown) were used to identify Fos and CTb immunoreactivity, respectively. After labeling, sections were mounted, rinsed in 50% ethanol and coverslipped. Cells that expressed hM_4Di were identified using immunodetection with anti-GFP antibody, which also labels mCitrine (the reporter co-expressed with hM_4Di) and quantified in epifluorescent photomicrographs (Colwill and Graslund, 2011). Immunolabeling for mCitrine was necessary for signal detection due to low/insufficient endogenous fluorescence. These sections were placed on slides and coverslipped with VectaShield containing DAPI (1.5 µg/ml). For six subjects in Experiment 2 additional brain sections were also immunolabeled for the neuronal marker, NeuN. Counts of NeuN-labeled cells were then used in combination with adjacent DAPI-sections to estimate the proportion of cells in the mOT that were neuronal.

Specific procedures for each experiment

Experiment 1: *Identification of Brain Regions That Project to the mOT and Are Activated By Opposite-Sex Odors.* A pilot study involving 3 subjects with unilateral injections of the retrograde tracer, CTb, in the rostral mOT found that there are negligible contralateral projections to the mOT. Therefore, mice were given bilateral injections of

CTb into the rostral mOT with the goal of examining only the ipsilateral hemisphere with the most accurate injection. Five days after CTb injections, behavioral estrus was induced (E_2+P) and mice were exposed to either testes-intact male soiled bedding/urine, estrous female soiled bedding/urine, or clean bedding/water prior to sacrifice. Brains were removed and subsequently processed for CTb and Fos double-labeling. Because Fos labeling may be compromised in neurons at injection sites, analysis of Fos induction in rostral mOT and lateral olfactory tubercle (lOT) could only be made in hemispheres where CTb injections missed these areas. Thus, mice with inaccurate or absent CTb deposits bilaterally (n=12) and/or appreciable spread of tracer into adjacent regions (n=4) were excluded from analysis of retrograde CTb labeling, but some of these mice were included in the analysis of mOT and lOT Fos expression. These missed injections were either very dorsal or lateral to the mOT, so it is unlikely that Fos induction in mOT neurons was perturbed in these cases. For brain regions outside of the injection sites, two different types of neuronal cell body labeling were quantified without knowledge of treatment group: (1) mOT-projecting, but not odor activated (CTb-labeled only); (2) both mOT-projecting and odor activated (CTb/Fos double-labeled). CTb and Fos labeling were defined based on differences in color and cellular localization (Fos: black, nucleus; CTb: brown, cytoplasm) using a light microscope with a 40x (oil) objective. Fos^+ and CTb^+ cells were counted in 21 forebrain regions in a standard (300^2 μm) counting area using the cell counter plugin in ImageJ (Schneider et al., 2012) and averaged from two non-overlapping tissue sections for each of the brain regions for each subject (Figs 1*A*-*H*). The percentage of CTb^+ cells that co-expressed Fos was calculated from the average of two tissue sections in each of 13 forebrain regions where CTb/Fos co-labeling was

observed. Comparisons between the 3 odor exposure groups (i.e., clean, male-soiled, or female-soiled bedding) were carried out using separate 1-way ANOVAs run for each of the 23 brain regions for Fos alone and 13 brain regions for CTb/Fos co-labeling. Because the VTA and MeA were designated a priori as areas of interest, the alpha level for statistical significance of the omnibus F-tests for these areas was set at 0.05. For ANOVAs run for all other brain regions, alpha was adjusted using the Benjamini-Hochberg correction (Benjamini and Hochberg, 1995). For ANOVAs where the omnibus F-test was significant, differences between odor exposure groups were subsequently examined by *post hoc* Student–Newman–Keuls tests.

Experiment 2*: DREADD-Induced Silencing of mOT Neurons.* Ovariectomized, E_2-treated subjects were given bilateral injections of either sterile PBS (vehicle) or virus containing the hM_4Di construct into the rostral mOT. Only subjects with bilateral hM_4Di infections centered in the rostral mOT (n=7) were used for analysis along with vehicle-injected controls (n=12). Subjects with significant viral spread into adjacent nuclei bilaterally (n=4), or those lacking detectable infection in one or both hemispheres (n=7) were excluded from behavioral analysis. Behavioral testing commenced three weeks after infection. Subjects received in the following order locomotor testing, *Volatiles Only* odor preference testing, *Volatiles+Nonvolatiles* odor preference testing, odor discrimination tests, and cookie odor preference tests. Each type of test was conducted once with and once without CNO treatment (counterbalanced). Either four days (for the first three test types) or two days (the final two test types) intervened before the next type of test. Finally, two days after the cookie test, subjects were exposed to volatile male

356 odors in either the presence or absence of CNO treatment, whereupon they were
357 sacrificed by perfusion 90 min after exposure onset. Brains were removed, cryosectioned
358 and processed for immunolabeling of Fos protein. Although mice could be tested both
359 with and without CNO present in the behavioral studies, subjects could receive only one
360 or the other treatment prior to sacrifice for Fos analysis. Because DREADD infections in
361 each hemisphere of a subject are distinct, Fos was analyzed in both hemispheres of each
362 subject and 'hemisphere' was used as the unit of analysis. Fos counts within the infected
363 rostral mOT zone were averaged from two non-overlapping sections of each hemisphere.
364 The mean number of Fos^+ cells in hemispheres from each group was compared using a
365 two-way ANOVA followed by a Student–Newman–Keuls *post hoc* test.
366 DREADD infection rates were determined using additional sections that were
367 immunolabeled for mCitrine and co-stained with DAPI. The total number of $mCitrine^+$
368 neurons divided by the total number of $DAPI^+$ cells counted in 3 non-overlapping
369 sections (rostral to caudal) of the rostral mOT were computed for each subject. Because
370 DAPI labels neuronal as well as non-neuronal nuclei, a separate estimate of neuronal
371 infection in the mOT was made. For this analysis, three tissue sections (rostral,
372 intermediate, and caudal mOT) that were adjacent to sections in which DAPI counts were
373 made were identified from six subjects in the study. These sections were immunolabeled
374 with NeuN, and the proportion of $NeuN^+$: $DAPI^+$ cells in the mOT were computed for
375 each set of adjacent sections. These values were then averaged for each subject and
376 expressed as the mean ±SEM for the six animals.
377
378 **Results:**

Experiment 1

To determine whether mOT neurons are activated by volatile odors in estrous female mice, E_2+P-treated subjects were exposed to volatiles from clean bedding, estrous female bedding or intact male bedding, and forebrains were immunostained for Fos protein (Fig. 2*A*-*C*). In the medial ($F_{2,22} = 9.9$, P=0.001[a]), but not lateral ($F_{2,22} = 1.3$, P=0.300[b]), olfactory tubercle, male odors increased neuronal Fos induction relative to female or control odors (Fig. 2*D*). This male urinary odor-induced increase in Fos protein was not confined to a specific layer of the mOT. Rather, there was an apparent increase in Fos expression in both the dense cell layer and multiform layer, which includes portions of the ventral pallidum and the islands of Calleja. Selective Fos expression specifically to male, but not to estrous female volatile odors was also found in the following regions: shell of the Acb (AcbSh), ventral tegmental area (VTA), anterior (MeA), posterodorsal (MePD) and posteroventral (MePV) portions of the Me, the posteromedial cortical amygdala (PMCo) and the posteroventral portion of piriform cortex (vpPC). A number of areas responded equally to odors from males or females, while in other regions, there was no Fos induction in response to either odor compared to clean bedding (Table 1).

The retrograde tracer CTb was used to identify brain regions that send axonal projections to the mOT. Evaluation of CTb injection sites indicated that tracer extended from rostral to caudal regions of the mOT (Fig. 3*A,B*). Back-labeled CTb^+ cell bodies were found in many ventral forebrain regions. (Fig. 3*C*). The densest labeling occurred in 'main olfactory' recipient amygdaloid and cortical nuclei. Regions of the 'vomeronasal amygdala' and structures associated with the mesolimbic dopamine system

were also labeled. To examine whether any of these mOT-projecting regions were activated by urinary volatiles, double-labeled sections (Fig. 4*C,F*) were analyzed to determine the extent of Fos (nucleus) and CTb (cytoplasm) co-localization. Of the 13 forebrain regions analyzed (Fig. 4*I*), exposure to male, but not female volatile chemosignals resulted in significant CTb/Fos co-labeling only in the Me and VTA (Fig. 4*A-I*, Me: $F_{2,25} = 4.4$, $P=0.023^{x}$; VTA: $F_{2,25} = 4.9$, $P=0.017^{y}$).

Experiment 2

Behavior. DREADD-induced silencing of the mOT was examined for effects on olfactory behavior. Preference for testes-intact male vs estrous female urinary volatiles was abolished in hM$_4$Di+CNO subjects ($P=0.012$), whereas preference for male chemosignals was maintained in hM$_4$Di+Saline, Vehicle+CNO, and Vehicle+Saline subjects (Fig. 5*A*) (main effect of Drug Treatment [$F_{1,37} = 6.0$; $P=0.026^{z}$] and Drug Treatment X Infection Type interaction [$F_{1,37} = 6.7$; $P=0.019^{aa}$] on odor investigation difference scores). Similar effects were observed when direct nasal contact with the urinary stimulus was permitted (Fig. 5*B*), such that preferences were observed for testes-intact male over estrous female urine in the hM$_4$Di+Saline, Vehicle+CNO, and Vehicle+Saline groups, but not in the hM$_4$Di+CNO females (Infection Type X Drug Treatment interaction [$F_{1,37} = 4.5$; $P=0.048^{bb}$], $P<0.02$, SNK *post hoc* tests). Total time spent investigating urinary volatiles depended on Drug Treatment (Fig. 5*C*) ($F_{1,37} = 8.4$; $P=0.01^{cc}$), an effect that appears to be driven mostly by reduced investigation of male chemosignals by hM$_4$Di+CNO subjects. No group differences in total investigation times were observed when direct nasal access

to the urinary stimulus was permitted (Fig. 5*D*) (Drug Treatment: P=0.969[dd]; Infection Type: P=0.589[ee]; Interaction: P=0.934[ff]).

In the odor discrimination task administered to ensure that DREADD-induced neuronal silencing in the mOT had no effect on subjects' ability to discriminate between the odors tested, all groups dishabituated from the final presentation of water to the first presentation of estrous female urine, as well as from the final presentation of estrous female urine to the first presentation of testes-intact male urine (Fig 6*A*, all $P \leq 0.014$[gg-nn]). Similarly, there were no group differences in the amount of time investigating either the first presentation of estrous female urine (Main effects: $P \geq 0.16$[oo-pp]; Interaction: P=0.323[qq]) or the first presentation of testes-intact male urine (Main effects: $P \geq 0.$[225rr-ss]; Interaction: P=0.750[tt]). All groups also strongly preferred to investigate cookie odor volatiles vs mineral oil vehicle ($P \leq 0.013$[uu-xx]), suggesting that reduced motivation to investigate male urinary odors in hM$_4$Di+CNO subjects is not generalized to food odors (Fig. 6*B*). Finally, no significant differences were found between groups in mean distance traveled in a locomotor test (Fig. 6*C*, Main effects: $P \geq 0.146$[yy-zz]; Interaction: P=0.364[aaa]), indicating that neither CNO nor hM$_4$Di receptor expression affected subjects' motor function.

Localization of hM$_4$Di Infection. A typical site where mOT infections were seen is shown for a representative subject in a Nissl stained section (Fig 7*A-A'*). Expression of the DREADD construct in the rostral mOT of an adjacent section from this animal is shown using low magnification epifluorescent (Fig. 7*B*) and high magnification confocal microscopy (Fig. 7*B'*) after immunolabeling for mCitrine. Fig 7*C* depicts boundaries

447 traced around mCitrine$^+$ neurons in three rostral mOT sections from each hemisphere of
448 all subjects (n=7). Sparse, errant mCitrine$^+$ cell bodies found outside of the border of the
449 primary mOT infection are also shown. The majority of infected neurons were located in
450 the rostral mOT, although infections often spread to include more caudal regions of the
451 mOT. Minor bilateral viral spread outside of the mOT was in some cases observed along
452 the border of the lateral ventricles, in the navicular postolfactory nucleus, the ventral
453 accumbens shell (AcbSh), in the caudal ventral tenia tecta (VTT) and in the nucleus of
454 the vertical limb of the diagonal band (VDB). Significant unilateral spread from the
455 caudal mOT into the VDB and/or the AcbSh was observed in 3 subjects, but these
456 animals were retained in the study since these areas were unaffected in the contralateral
457 hemisphere. Few mCitrine$^+$ cell bodies were observed elsewhere in the brain, as adeno-
458 associated viruses are transported predominantly in the anterograde direction (Harris et
459 al., 2012). The only region outside of the targeted infection area where mCitrine$^+$ cell
460 bodies were regularly found was in piriform cortex (PC), although infection levels were
461 very low (~5-15 mCitrine$^+$ cell bodies/section). mCitrine$^+$ fibers were observed in many
462 regions known to receive input from the mOT, including the MOB, anterior olfactory
463 nucleus (AON), PLCo, anterior and posterior PC, and the VP, with sparse labeling
464 observed in the caudate putamen (CPu) and VTA.
465
466 *Estimate of hM$_4$Di Infection Rates.* The proportion of DAPI$^+$ cells that coexpressed
467 mCitrine was determined for the infected regions traced in the three sections shown for
468 each subject in Fig. 7*C*. These measures for each section were averaged within and
469 across subjects to obtain a mean ± SEM hM$_4$Di infection rate of 20 ± 2%. From a

separate analysis of NeuN and DAPI labeling in sections from six subjects it was determined that 78 ±7.5% of DAPI-labeled cells in the mOT are neurons, accordingly the proportion of the mOT neuronal population infected by hM_4Di is likely greater than 20%.

Odor-induced Fos. To confirm the efficacy of DREADD inhibition *in vivo*, female subjects were exposed to volatile chemosignals from testes-intact males prior to sacrifice (Fig. 8*A-B'*). In hM_4Di+CNO subjects, there was a significant reduction in mOT Fos expression compared to all other groups (Fig. 8*C*), suggesting that neuronal activity is diminished by CNO-induced DREADD receptor activation, and not by CNO alone or DREADD infection alone (main effects of Drug Treatment [$F_{1,41} = 15.4$; $P<0.001^{bbb}$] and Infection Type [$F_{1,41} = 15.5$; $P<0.001^{ccc}$], and interaction of Infection Type X Drug Treatment [$F_{1,41} = 9.7$; $P=0.003^{ddd}$]). Importantly, decreased Fos expression has been used previously to confirm CNO-induced neuronal silencing in hM_4Di-infected brain regions (Sasaki et al., 2011; Ferguson et al., 2011; Michaelides et al., 2013; Pei et al., 2014).

Discussion:

The present results indicate that neuronal activity in the mOT plays an essential role in motivating female mice to investigate male odors, providing evidence that the mOT is part of a circuit that regulates innate attraction of mice for urinary odors. When the rostral mOT of hM_4Di-infected estrous females was silenced with CNO, preference for intact male over estrous female urinary volatiles and nonvolatiles was abolished, whereas preference persisted when subjects were treated with saline. Furthermore, CNO

493 treatment had no effect on vehicle-injected subjects. These findings, along with previous
494 findings (DiBenedictis et al., 2014b; Agustin-Pavon et al., 2014), highlight the
495 importance of the ventral striatum in the 'hardwired' circuitry that underlies behavioral
496 preferences for opposite-sex pheromones—a first step in mate recognition leading to
497 successful reproduction.

498 The mOT has been linked to drug reinforcement (Ikemoto, 2010) as well as to
499 olfactory perception (Payton et al., 2012). Thus, it is possible that the decrements we
500 observed in investigation of urinary odors during CNO-induced mOT inhibition were due
501 to sensory deficits in odor detection, or to interference with processing of odors from the
502 direct projections of the MOB to the mOT. However, mOT-hM_4Di^+ subjects treated with
503 CNO were able to perceive differences between the urinary odors tested, as indexed by a
504 robust dishabituation response to the first presentation of each odor. This result suggests
505 that reduced preference for male odors did not result from females' inability to
506 discriminate male and female urinary odors. Instead, the mOT may modulate urinary
507 odor-driven behaviors by attributing salience to these odors, either locally or via its
508 reward-associated projection targets. This latter view is supported by the recent report
509 (Gadziola et al., 2015) that activity of OT neurons increased upon presentation of various
510 non-pheromonal odors that predicted the delivery of a water reward to thirsty mice. In
511 the present study, CNO treated subjects retained their preference for volatile cookie odors
512 over mineral oil vehicle, indicating that the mOT may not influence females' motivation
513 to investigate food odors. Finally, all subjects displayed equivalent levels of locomotor
514 activity regardless of whether or not they received CNO. This rules out any possibility
515 that deficits in preferences for male odors were due to subjects' physical inability to

approach/investigate odor stimuli.

Volatile components of odors are detected by the main olfactory system. In this pathway, sensory neurons in the main olfactory epithelium send axonal projections to the MOB, which in turn radiates information via mitral/tufted cell projection neurons to downstream targets, including olfactory cortical structures and portions of the amygdala referred to as the 'olfactory amygdala' as well as nuclei of the 'vomeronasal amygdala,' and particularly the medial amygdala (Kang et al., 2009). Lesions of the main olfactory epithelium eliminate male urinary volatile-induced Fos expression in olfactory targets of the female mouse forebrain (Martel and Baum, 2007), and reduce lordosis behavior and attraction male pheromones (Keller et al., 2006). These findings suggest that the main olfactory system plays an essential role in processing male pheromonal odors in female mice. In the present study, we also found a selective activation of the mOT (i.e., increased Fos expression) of females in response to volatiles from male-, but not from female-soiled bedding, implicating the mOT in the circuitry that processes innately attractive, opposite-sex odors. Notably, the AcbSh also responded preferentially to opposite-sex odors and receives dopaminergic inputs from the VTA. In our study, a small number of hM_4Di-infected cell bodies was detected unilaterally in the ventromedial AcbSh of 3 subjects; this could have contributed to the deficit in male odor preference displayed by subjects with bilateral hM_4Di infections of the mOT after CNO treatment. Although the AcbSh receives only sparse direct inputs from the Me (DiBenedictis et al., 2014a; Pardo-Bellver et al., 2012), it is strongly interconnected with the mOT. Thus, the AcbSh may also be involved in aspects of urinary odor-driven sociosexual motivation. More work is needed to test this hypothesis.

539 Deficits in the investigation of opposite-sex odors during DREADD-induced
540 inhibition of mOT neuronal activity occurred not only in tests in which only urinary
541 volatiles were available, but also in tests during which both volatile and non-volatile
542 urinary chemosignals could be detected. Non-volatile chemosignals are processed by the
543 accessory olfactory system (Luo and Katz, 2004), and indeed, surgical removal of the
544 VNO reduced the investigation of opposite-sex urinary odors in female mice (Martel and
545 Baum 2009b). Thus, our present results show that chemosignals in testes-intact male
546 urine, whether processed by the main and/or accessory olfactory systems, require input to
547 the mOT to render them attractive to females.

548 An initial indication that the mOT may play an essential role in interpreting the
549 salience of pheromonal cues in female mice came from the report (Agustin-Pavon et al.,
550 2014) that bilateral electrolytic lesions of the medioventral striato-pallidum (mvStP), but
551 not of the posterolateral striato-pallidum, eliminated females' preference to investigate
552 male vs female chemosignals. Our results focus attention on the mOT, a subdivision of
553 the larger mvStP, as the critical site in mediating the rewarding effects of opposite-sex
554 pheromones, just as the mOT as opposed to the lateral part of the OT has been implicated
555 in drug reward (Ikemoto, 2010). Our results using DREADD methodology show for the
556 first time that silencing activity in the mOT eliminated females' preference to investigate
557 male pheromones without compromising their ability to discriminate between these odors
558 or reducing females' motivation to investigate food odors.

559 We found that a subset of neurons projecting to the mOT from the MeA and VTA
560 showed preferential induction of Fos in response to male- compared to female-bedding
561 odors. This suggests that the MeA and VTA are key regions driving the selective

562 activation of the rostral mOT during exposure to volatile chemosignals from testes-intact
563 males. In corroboration, it was previously found that the MeA densely innervates the
564 mOT (DiBenedictis et al., 2014a; Pardo-Bellver et al., 2012). Both anterior and posterior
565 segments of the Me may also drive activity in the mOT via indirect polysynaptic inputs
566 involving the pBNST and PMCo (Novejarque et al., 2011; Ubeda-Banon et al., 2008).
567 The VTA provides dopaminergic innervation to the ventral striatum, including the Acb,
568 VP and OT complex, and neurons in the VTA express Fos in response to opposite-sex
569 chemosignals (Moncho-Bogani et al., 2005; Martel & Baum 2009a; Kang et al., 2009)
570 thereby implicating this region in the processing of salient olfactory information. It has
571 also been shown that dopaminergic modulation of the mAcb and mOT is necessary for
572 the display of male urinary odor-driven courtship behaviors in estrous female mice
573 (DiBenedictis et al., 2014b), further implicating the VTA in pheromone reinforcement.
574 The mOT is a component of the VS, and receives pheromonal input from
575 limbic/amygdaloid structures. Thus, our results are consistent with the hypothesis that
576 neuronal activity in the mOT modulates urinary odor-driven motivated behaviors in mice.
577 DREADD methodology offers several useful advantages for studying olfactory
578 behaviors. It is reversible, so (to our knowledge) there is no damage to temporarily
579 silenced neurons, and it enables animals to be tested repeatedly and in alternating control
580 and mOT-inhibited conditions. Moreover, infected neurons are easily identified and
581 quantified using a co-expressed reporter gene. The level of viral infection in our study
582 was sufficient to produce both functional deficits in odor-induced activation of Fos as
583 well as in the investigation of opposite-sex chemosignals. Additionally, we calculated
584 infection rates based on a DAPI counterstain—which labels nuclear DNA in both neurons

and glia (Kapuscinski, 1995)—so it is likely that the proportion of neurons infected in the present study was higher than the DAPI-based estimate of ~20%. In a separate examination we conducted using brain sections that were labeled with DAPI and the neuron-specific marker NeuN, ~78% of the total number of DAPI-labeled cells in the mOT were found to be neurons. An estimate of the proportion of neurons infected by the DREADD virus may therefore be closer to 25%.

Retrograde labeling of cell bodies in subjects given CTb injections was found in many forebrain regions known to innervate the mOT (Newman and Winans, 1980). We found that the majority of inputs to the mOT derived from 'main olfactory' recipient cortical nuclei, such as the PC, although a fair number of back-labeled cell bodies were also observed in the VTA and BLA. 'Vomeronasal' recipient nuclei, including the MeA and PMCo, also targeted the mOT, though to a much lesser extent than PC. These results are consistent with other studies suggesting that the mOT is interconnected with olfactory structures that include the MOB, PC, and the 'vomeronasal amygdala' as well as hypothalamic, hippocampal, and reward-associated brain regions such as the Acb, LS, VTA, VP, and CPu, among others (Wesson & Wilson, 2011). Future studies should exploit genetically guided, cell-specific techniques to activate or inhibit particular mOT neuronal populations in behaving animals in order to further specify the role of this region in mediating the effects of pheromones on courtship behaviors.

References:

Agustin-Pavon C, Martinez-Garcia F, Lanuza E (2014) Focal lesions within the ventral striato-pallidum abolish attraction for male chemosignals in female mice. Behav Brain Res 259:292-6.

Armbruster BN1, Li X, Pausch MH, Herlitze S, Roth BL (2007) Evolving the lock to fit the key to create a family of G protein-coupled receptors potently activated by an inert ligand. Proc Natl Acad Sci (12):5163-68.

Baker DA, Fuchs RA, Specio SE, Khroyan TV, Neisewander JL (1998) Effects of intraaccumbens administration of SCH-23390 on cocaine-induced locomotion and conditioned place preference. Synapse 30:181–93.

Benjamini Y, Hochberg Y (1995) Controlling the false discovery rate: a practical and powerful approach to multiple testing. J Royal Stat Soc, Series B. 57:289–300.

Brock O, Baum MJ, Bakker J (2011) The development of female sexual behavior requires prepubertal estradiol. J Neurosci 31:5574-8.

Cassataro D, Bergfeldt D, Malekain C, Van Snellenberg JX, Thanos PK, Fishell G, Sjulson L (2014) Reverse pharmacogenetic modulation of the nucleus accumbens reduces ethanol consumption in a limited access paradigm. Neuropsychopharmacol 39:283-90.

Choi GB, Dong HW, Murphy AJ, Valenzuela DM, Yancopoulos GD, Swanson LW, et al. (2005) Lhx6 delineates a pathway mediating innate reproductive behaviors from the amygdala to the hypothalamus. Neuron 46:647–60.

Colwill K, Graslund S (2011) A roadmap to generate renewable protein binders to the human proteome. Nat Methods 8:551-8.

Cullinan WE, Herman JP, Battaglia DF, Akil H, Watson SJ (1995) Pattern and time course of immediate early gene expression in rat brain following acute stress. Neurosci 64:477-505.

DiBenedictis BT, Helfand AI, Baum MJ, Cherry JA (2014a) A quantitative comparison of the efferent projections of the anterior and posterior subdivisions of the medial amygdala in female mice. Brain Res 1543:101-8.

DiBenedictis BT, Olugbemi AO, Baum MJ, Cherry JA (2014b) 6-hydroxydopamine lesions of the anteromedial ventral striatum impair opposite-sex urinary odor preference in female mice. Behav Brain Res 274:243-7.

Farrell MS, Roth BL (2013) Pharmacosynthetics: reimagining the pharmacogenetic approach. Brain Res 1511:6-20.

649 Farrell MS, Pei Y, Wan Y, Yadav PN, Daigle TL, Urban DJ et al., (2013) A Gαs
650 DREADD mouse for selective modulation of cAMP production in striatopallidal neurons.
651 Neuropsychopharmacol 38:854-62.
652
653 Ferguson SM, Eskenazi D, Ishikawa M, Wanat MJ, Phillips PE, Dong Y, et al., (2011)
654 Transient neuronal inhibition reveals opposing roles of indirect and direct pathways in
655 sensitization. Nat Neurosci 14:22-4.
656
657 FitzGerald BJ, Richardson K, Wesson DW (2014) Olfactory tubercle stimulation alters
658 odor preference behavior and recruits forebrain reward and motivational centers. Front
659 Behav Neurosci 8:81.
660
661 Franklin KBJ, Paxinos G (2008) The mouse brain in stereotaxic coordinates, 3rd ed.
662 Academic Press, California.
663
664 Gadziola MA, Tylicki KA, Christian DL, Wesson DW (2015) The olfactory tubercle
665 encodes odor valence in behaving mice. J Neurosci 35:4515-27.
666
667 Garner AR, Rowland DC, Hwang SY, Baumgaertel K, Roth BL, Kentros C et al., (2012)
668 Generation of a synthetic memory trace. Science 335:1513-6.
669
670 Harris JA, Oh SW, Zeng H (2012) Adeno-associated viral vectors for anterograde axonal
671 tracing with fluorescent proteins in nontransgenic and cre driver mice. Curr Protoc
672 Neurosci Apr; Chapter 1:Unit 1.20.1-18.
673
674 Heinz A, Beck A, Gusser SM, Grace AA, Wrase J (2009) Identifying the neural circuity
675 of alcohol craving and relapse vulnerability. Addict Biol 14:108-18.
676
677 Ikemoto S (2010) Brain reward circuitry beyond the mesolimbic dopamine system: a
678 neurobiological theory. Neurosci Biobehav Rev 35:125-50.
679
680 Ikemoto S (2003) Involvement of the olfactory tubercle in cocaine reward: intracranial
681 self-administration studies. J Neurosci 23:9305-11.
682
683 Ikemoto S, Sharpe LG (2001) A head-attachable device for injecting nano-liter volumes
684 of drug solutions into brain sites of freely moving rats. J Neurosci Methods 110:135–40.
685
686 Ikemoto S, Qin M, Liu ZH (2005) The functional divide for primary reinforcement of D-
687 amphetamine lies between the medial and lateral ventral striatum: Is the division of the
688 accumbens core, shell and olfactory tubercle valid? J Neurosci 25:5061-65.
689
690 Isles AR, Baum MJ, Ma D, Szeto A, Keverne EB, Allen ND (2002) A possible role for
691 imprinted genes in inbreeding avoidance and dispersal from the natal area in mice. Proc
692 Biol Sci 269:665-70.
693
694 Kang N, Baum MJ, Cherry JA (2009) A direct main olfactory bulb projection to the

695 'vomeronasal' amygdala in female mice selectively responds to volatile pheromones
696 from males. Eur J Neurosci 29:624–34.
697
698 Kapuscinski J (1995) DAPI: a DNA-specific fluorescent probe. Biotech Histochem
699 70:220-33.
700
701 Keller M, Douhard Q, Baum MJ, Bakker J (2006) Destruction of the main olfactory
702 epithelium reduces female sexual behavior and olfactory investigation in female mice.
703 Chem Senses 31:315-23.
704
705 Koob GF, Volkow ND (2010) Neurocircuitry of addiction. Neuropsychopharmacol
706 35:217-38.
707
708 Liao RM, Chang YH, Wang SH, Lan CH (2000) Distinct accumbal subareas are involved
709 in place conditioning of amphetamine and cocaine. Life Sci 67:2033–43.
710
711 Luo M, Katz LC (2004) Encoding pheromonal signals in the mammalian vomeronasal
712 system. Curr Opin Neurobiol 14:428-34.
713
714 Martel KL, Baum MJ (2007) Sexually dimorphic activation of the accessory, but not the
715 main, olfactory bulb in mice by urinary volatiles. Eur J Neurosci 26:463–75.
716
717 Martel KL, Baum MJ, (2009a) A centrifugal pathway from to the mouse accessory
718 olfactory bulb from the medial amygdala conveys gender-specific volatile pheromonal
719 signals. Eur J Neurosci 29:368–76.
720
721 Martel KL, Baum MJ, (2009b) Adult testosterone treatment but not surgical disruption of
722 vomeronasal function augments male-typical sexual behavior in female mice. J Neurosci
723 29:7658–66.
724
725 McGregor A, Roberts DC (1993) Dopaminergic antagonism within the nucleus
726 accumbens or the amygdala produces differential effects on intravenous cocaine self-
727 administration under fixed and progressive ratio schedules of reinforcement. Brain Res
728 624:245–52.
729
730 Michaelides M, Anderson S-A R, Ananth M, Smirnov D, Thanos P, Neumaier J et al.,
731 (2013) Whole-brain circuit dissection in free-moving animals reveals cell-specific
732 mesocorticolimbic networks. J Clin Invest 123:5342-50.
733
734 Moncho-Bogani J, Martinez-Garcia F, Novejarque A, Lanuza E (2005) Attraction to
735 sexual pheromones and associated odorants in female mice involves activation of the
736 reward system and basolateral amygdala. Eur J Neurosci 21:2186–98.
737
738 Newman R, Winans SS (1980) An experimental study of the ventral striatum of the
739 golden hamster. II. Neuronal connections of the olfactory tubercle. J Comp Neurol
740 (2):193-212.

741
742 Novejarque A, Gutierrez-Castellanos N, Lanuza E, Martınez-Garcıa F (2011)
743 Amygdaloid projections to the ventral striatum in mice: direct and indirect chemosensory
744 inputs to the brain reward system. Front Neuroanat 5 http://dxdoi.org/10.3389/
745 fnana.2011.00054.
746
747 Pardo-Bellver C, Cádiz-Moretti B, Novejarque A, Martínez-García F, Lanuza E (2012)
748 Differential efferent projections of the anterior, posteroventral, and posterodorsal
749 subdivisions of the medial amygdala in mice. Front Neuroanat 6:33 doi:
750 10.3389/fnana.2012.00033.
751
752 Payton CA, Wilson DA, Wesson DW (2012) Parallel odor processing by two
753 anatomically distinct olfactory bulb target structures. PLoS One 7:e34926 doi:
754 10.1371/journal.pone.0034926.
755
756 Pei H, Sutton A, Burnett K, Fuller P, Olsen D (2014) AVP neurons in the paraventricular
757 nucleus of the hypothalamus regulate feeding. Molec Metabolism 3:209-215 doi:
758 10.1016/j.molmet.2013.12.006.
759
760 Penagarikano O, Lazaro MT, Lu X-H, Gordon A, Dong H, Lam HA et al., (2015)
761 Exogenous and evoked oxytocin restores social behavior in the Cntnap2 mouse model of
762 autism. Sci Transl Med 7:271ra8 doi: 10.1126/scitranslmed.3010257.
763
764 Roberts DCS, Corcoran ME, Fibiger HC (1977) On the role of ascending
765 catecholaminergic systems in intravenous self-administration of cocaine. Pharmacol
766 Biochem Behav 6:615-20.
767
768 Roberts DCS, Koob GF, Klonoff P, Fibiger HC (1979) Extinction and recovery of
769 cocaine self-administration following 6-hydroxydopamine lesions of the nucleus
770 accumbens. Pharmacol Biochem Behav 12:781-87.
771
772 Rodd-Henricks ZA, McKinzie DL, Li TK, Murphy JM, McBride WJ (2002) Cocaine is
773 self-administered into the shell but not the core of the nucleus accumbens of Wistar rats. J
774 Pharmacol Exp Ther 303:1216 –26.
775
776 Rogan SC, Roth BL (2011) Remote control of neuronal signaling. Pharmacol Rev
777 63:291-315.
778
779 Sasaki K, Suzuki M, Mieda M, Tsujino N, Roth B, Sakurai T (2011) Pharmacogenetic
780 modulation of orexin neurons alters sleep/wakefulness states in mice. PLoS One
781 6:e20360. doi:10.1371/journal.pone.0020360.
782
783 Schneider CA, Rasband WS, Eliceiri KW (2012) NIH Image to ImageJ: 25 years of
784 image analysis. Nat Methods 9:671-75.
785
786 Schwob JE, Price JL (1984a) The development of axonal connections in the central

olfactory system of rats. J Comp Neurol 223:177–202.

Stachniak TJ, Ghosh A, Sternson SM (2014) Chemogenetic synaptic silencing of neural circuits localizes a hypothalamus→midbrain pathway for feeding behavior. Neuron 82:797-808.

Ubeda-Banon I, Novejarque A, Mohedano-Moriano A, Pro-Sistiaga P, Insausti R, Martinez-Garcia F, Lanuza E, Martinez-Marcos A (2008) Vomeronasal inputs to the rodent ventral striatum. Brain Res Bull 75:467–73.

Wang H, Duclot F, Liu Y, Wang ZX, and Kabbaj M (2013) Histone deacetylase inhibitors facilitate partner preference formation in female prairie voles. Nat Neurosci 16:919-24.

Wesson DW, Wilson DA (2010) Smelling sounds: olfactory-auditory sensory convergence in the olfactory tubercle. J Neurosci 30:3013–21.

Wesson DW, Wilson DA (2011) Sniffing out the contributions of the olfactory tubercle to the sense of smell: hedonics, sensory integration, and more? J Neurobio Rev 35:655–668.

White LE (1965) Olfactory bulb projections of the rat. Anat Rec 152:465-79.

Figure legends:

Figure 1. Modified schematic from the mouse brain atlas of Franklin and Paxinos (2008) showing the forebrain regions in which Fos-IR, CTb-IR and Fos-IR+CTb-IR cells (light gray boxes; 300^2 μm) were counted. Counting regions (from left to right) included the medial (mOT) and lateral (lOT) olfactory tubercle (Fos only) ***(A)***, the shell (AcbSh) and core (AcbC) of the nucleus accumbens ***(B)***, the medial preoptic area (MPA), dorsal (daPC), intermediate (iaPC) and ventral (vaPC) anterior piriform cortex ***(C)***, posterior division of the bed nucleus of the stria terminalis (BNST) ***(D)***, anterior medial amygdala (MeA), anterior cortical amygdala (Aco), dorsal (dpPC), intermediate (ipPC), and ventral (vpPC) posterior piriform cortex ***(E)***, dorsomedial (VMHdm) and ventrolateral (VMHvl) divisions of the ventromedial hypothalamus, posterodorsal (MePD) and posteroventral (MePV) medial amygdala, basomedial (BMA) and basolateral (BLA) amygdala, and posterolateral cortical amygdala (PLCo) ***(F)***, posteromedial cortical amygdala (PMCo) ***(G)***, and ventral tegmental area (VTA) ***(H)***. Numerical values represent the distance in mm from bregma for each section (Franklin and Paxinos 2008).

Figure 2. Medial (mOT), but not lateral (lOT) olfactory tubercle neurons were selectively activated in female mice by volatiles emitted from opposite-sex (male) soiled bedding***. A-C,*** Representative photomicrographs depicting Fos protein immunoreactivity in the mOT of female subjects exposed to volatiles from clean bedding (CB) ***(A)***, estrous female soiled bedding (EFB) ***(B)*** and testes-intact male soiled bedding (IMB) ***(C)***. ***(D)*** Average number of Fos-immunoreactive (IR) cells (±SEM) observed in the medial and lateral olfactory tubercle in response to volatiles from clean bedding, estrous female

831 soiled bedding or testes-intact male soiled bedding. *P<0.01; **P<0.001 (SNK *post hoc*
832 tests following a significant overall ANOVA). In the legend, n refers to the number of
833 subjects in each group.
834
835 **Figure 3.** ***(A)*** Representative photomicrograph showing a cholera toxin B (CTb)
836 injection site in the mOT. ***(B)*** Schematic reconstruction of coronal sections of the largest
837 (black) and smallest (gray) injection site in female mice given CTb injections in the
838 mOT. Sections are ordered sequentially from anterior (left) to posterior (right), with the
839 numbers shown representing the distance in mm anterior to bregma for each section.
840 Adapted from Franklin and Paxinos (2008). ***(C)*** Mean (±SEM) number of back-labeled
841 CTb^+ cell bodies in various forebrain sites in female mice given CTb injections into the
842 mOT five days previously (n=30). AcbC, AcbSh, nucleus accumbens core, shell; VTA,
843 ventral tegmental area; MeA, MePD, MePV, anterior, posterodorsal and posteroventral
844 medial amygdala; pBNST, posterior bed nucleus of the stria terminalis; BMA, BLA,
845 basomedial and basolateral amygdala; Aco, PLCo, PMCo, antero, posterolateral,
846 posteromedial cortical amygdala; daPC, iaPC, vaPC, dpPC, ipPC, vpPC, anterodosal,
847 intermediate, ventral, posterodorsal, intermediate, ventral piriform cortex; MPA, medial
848 preoptic area; VMHvl, VMHdm, ventrolateral, dorsomedial portions of the ventromedial
849 hypothalamus.
850
851 **Figure 4.** A subset of retrogradely-labeled neurons in the anterior medial amygdala
852 (MeA) and ventral tegmental area (VTA) in female mice given a prior injection of CTb in
853 the mOT coexpressed Fos in response to opposite sex (male) volatile odors from soiled

bedding (IMB). ***A,B,*** Representative photomicrographs depicting back-labeled CTb^+ (brown) and Fos^+ (black) neurons in the MeA ***(A)*** and the VTA ***(B)***. White arrows point to neurons positive for CTb; black arrows point to neurons positive for Fos; grey arrows point to neurons positive for both CTb and Fos (CTb^+/Fos^+). ***C-H***, High magnification (100x) photomicrographs depicting colabeled (CTb^+/Fos^+) neurons demarcated by grey arrows in the MeA ***(C)*** and VTA ***(F)***, neurons positive for CTb only, demarcated by white arrows in the MeA ***(D)*** and VTA ***(G)*** and neurons positive for Fos only, demarcated by black arrows in the MeA ***(E)*** and VTA ***(H)***. ***I,*** Effect of volatiles emitted from soiled bedding on the expression of Fos in various forebrain neurons of estrous female mice that were retrogradely labeled by a prior injection of cholera toxin B (CTb) into the mOT. The mean percentage (±SEM) of CTb-labeled (mOT-projecting) cells that coexpressed Fos in response to volatiles from clean bedding, estrous female soiled bedding, or testes intact male soiled bedding is shown in 13 forebrain regions where Fos/CTb colocalization was observed. *$P \leq 0.05$ (SNK *post hoc* tests following a significant overall ANOVA). In the legend, 'n' refers to the number of subjects in each group. See Fig. 3 caption for definitions of brain region acronyms.

Figure 5. ***A, B,*** Effect of bilateral CNO-induced mOT silencing (hM_4Di+CNO) on the preference of ovariectomized, estradiol and progesterone-primed female mice to investigate urinary odors from estrous female versus testes-intact male mice presented simultaneously in subjects' home cage. ***(A)*** Subjects' preference for volatile urinary odors presented outside the home cage (Non-Contact – Volatiles Only) and ***(B)*** subjects' preference for volatile plus non-volatile urinary odors presented inside the home cage

(Nasal Contact – Volatiles+Nonvolatiles). Data are represented as the average (±SEM) time spent investigating intact male urine minus the time spent investigating estrous female urine for each group. Different letters above columns in each group indicate statistically significant differences from each other (2-way repeated measures ANOVA with one factor repetition followed by SNK *post hoc* test). The number of subjects in each group is given within columns in parentheses. ***C,D,*** Effect of bilateral CNO-induced mOT silencing (hM_4Di+CNO) on the total amount of time ovariectomized, estradiol and progesterone-primed female mice spent investigating urinary stimuli. ***(C)*** Total amount of time subjects spent investigating intact male + estrous female urinary volatiles (Non-Contact – Volatiles Only). ***(D)*** Total amount of time subjects spent investigating intact male plus estrous female urinary volatiles and non-volatiles (Nasal Contact – Volatiles+Nonvolatiles). Data are represented as the average (±SEM) time spent investigating intact male urine plus the average time spent investigating estrous female urine for each group ($P>0.05$, 2-way repeated measures ANOVA with one factor repetition). The number of subjects in each group is given within columns in parentheses.

Figure 6. ***A,*** Effect of bilateral CNO-induced mOT silencing (hM_4Di+CNO) on the ability of ovariectomized, estradiol-primed female mice to discriminate between testes-intact male and estrous female volatile urinary odors presented outside of the home cage (Volatiles Only). Each stimulus was presented three consecutive times. Estrous female vs testes-intact male urinary volatiles were reliably discriminated by all groups (Paired *t*-test comparisons of mean investigation times of third water vs first female urine, and

900 third female urine vs first male urine; *, +, #, **, $P<0.001$). No between group
901 differences in the level of investigation during the first presentation of estrous female
902 urine and the first presentation of intact male urine were observed ($P>0.05$, 2-way
903 repeated measures ANOVA with one factor repetition). ***B,*** Effect of bilateral CNO-
904 induced mOT silencing (hM_4Di+CNO) on the preference of ovariectomized, estradiol-
905 primed female mice to investigate volatiles emanating from cookie odor dissolved in
906 mineral oil versus mineral oil alone presented simultaneously in subjects' home cage.
907 Data are represented as the mean (±SEM) time spent investigating each odor (*, $P<0.01$,
908 paired *t*-test comparisons of mean investigation times for each odor). ***C,*** Effect of
909 bilateral CNO-induced mOT silencing (hM_4Di+CNO) on locomotion displayed by
910 ovariectomized, estradiol-primed female mice. Data are represented as the mean (±SEM)
911 distance traveled (in meters) in a 20 min open field test ($P>0.05$, 2-way repeated
912 measures ANOVA with one factor repetition). The number of subjects in each group is
913 given within columns in parentheses.
914
915 **Figure 7.** ***A,*** Low magnification (4x) Nissl stained photomicrograph of the brain tissue
916 section containing the medial ventral striatum depicted in ***(A')***, outlined by the boxed
917 region. The red dashed region outlines the mOT and the blue dashed region outlines the
918 lOT. ***A',*** Nissl stained photomicrograph depicting the medial portion of the ventral
919 striatum (medial nucleus accumbens and medial olfactory tubercle) in an adjacent section
920 of forebrain depicted in ***(B)***. The dashed region outlines the mOT. ***B,*** Epifluorescent
921 photomicrograph depicting hM_4Di infection in the rostral mOT, immunolabeled for the
922 coexpressed reporter, mCitrine. The dashed region outlines the mOT. White arrows

point to errant infected cell bodies found outside of the mOT, illustrated as colored dots outside of the traced regions in ***(C)***. ***B',*** Z-plane stacked confocal image showing mCitrine^{+} cell bodies and fibers magnified from the white, boxed region in ***(B)***. ***C,*** Modified schematic from the mouse brain atlas of Franklin and Paxinos (2008) illustrating regions where hM$_4$Di^{+} and DAPI^{+} cells were quantified. Different color tracings indicate the extent of bilateral hM$_4$Di infection within three rostral sections of the ventral striatum for each subject (n=7). Different color dots represent sparse, errant hM$_4$Di^{+} neurons found outside of densely infected (traced) region for each subject. Sections are ordered sequentially from anterior (top) to posterior (bottom), with numerical values representing the distance in mm anterior to bregma for each section. aca, anterior commissure; AcbSh, AcbC, nucleus accumbens shell and core; cc, corpus callosum; ICj, island of Calleja; lOT, lateral olfactory tubercle; mfb, medial forebrain bundle; mOT, medial olfactory tubercle; VDB, vertical limb of the diagonal band of Broca.

Figure 8. ***A,*** Photomicrograph depicting low Fos protein expression in response to male bedding volatiles in the mOT of a CNO-treated subject. ***A',*** high magnification photomicrograph of the boxed area shown in ***(A)***. ***B,*** Photomicrograph depicting augmented Fos protein expression in response to male bedding volatiles in the mOT of a saline-treated subject. ***B',*** high magnification photomicrograph of the boxed area in ***(B)*** showing Fos^{+} cell bodies. ***C,*** hM$_4$Di+CNO treated subject showed reduced Fos protein expression following exposure to testes-intact male soiled bedding volatiles compared to hM$_4$Di+Saline treated, Vehicle+CNO treated, and Vehicle+Saline treated subjects. ***(C)***

946 Mean number of Fos-immunoreactive cells (±SEM) observed in the mOT in response to
947 volatiles from testes intact male soiled bedding. Different letters above columns in each
948 group indicate statistically significant differences from each other (2-way repeated
949 measures ANOVA followed by SNK *post hoc* test). The number of hemispheres
950 examined for each group is given within columns in parentheses.

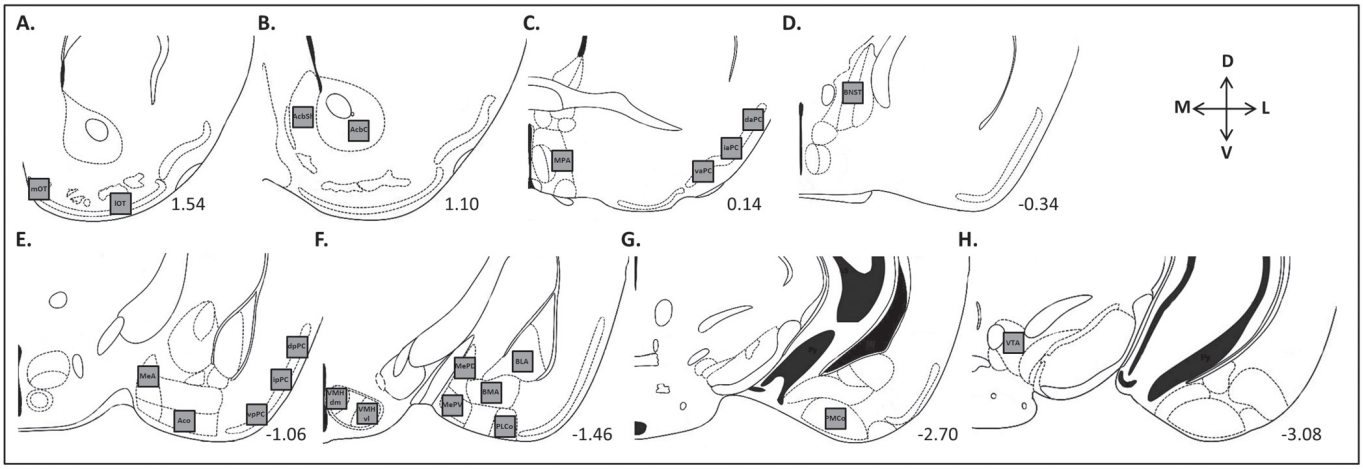

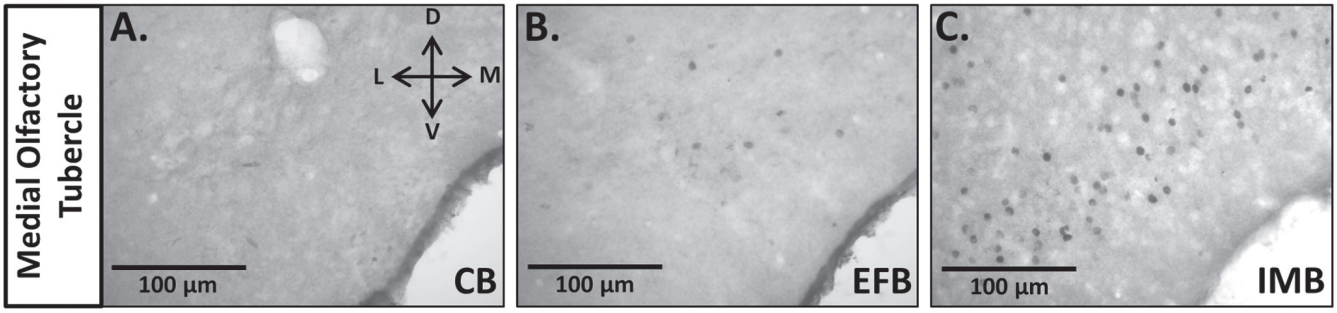

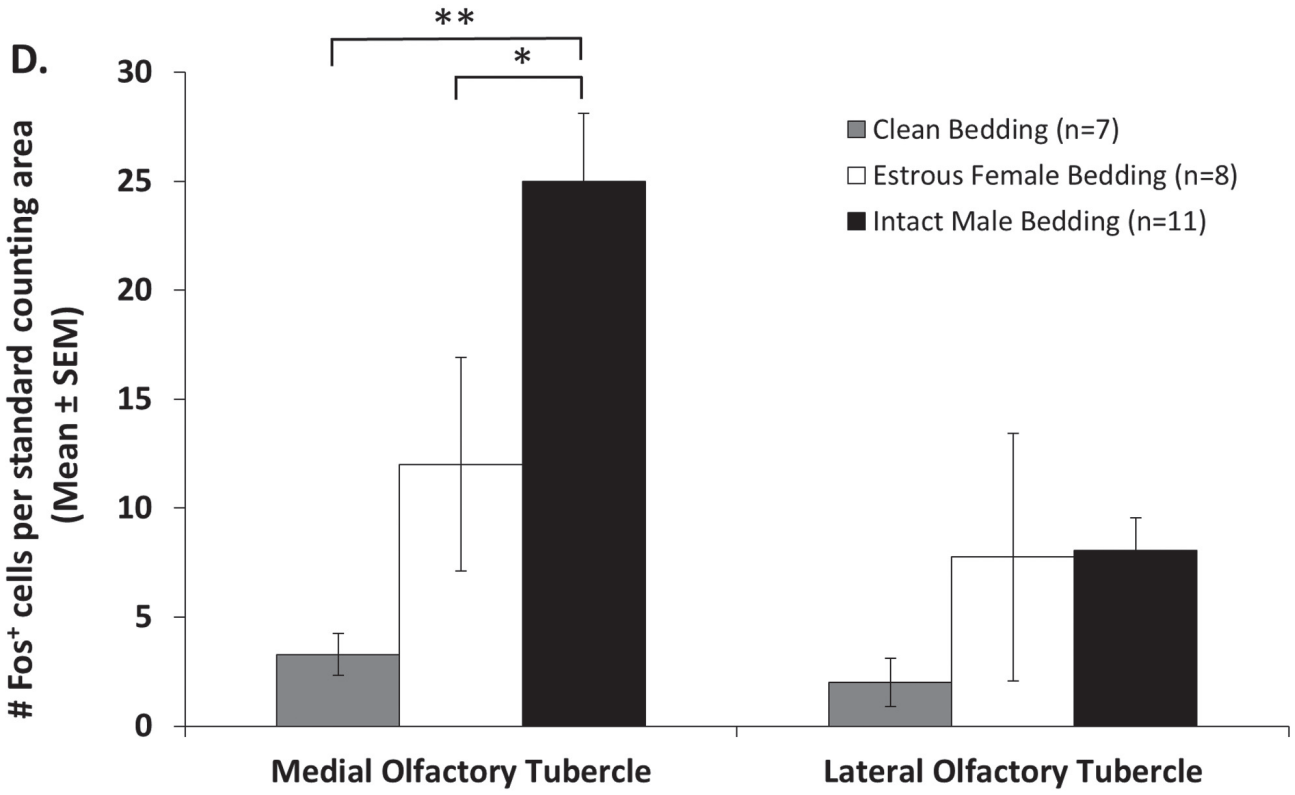

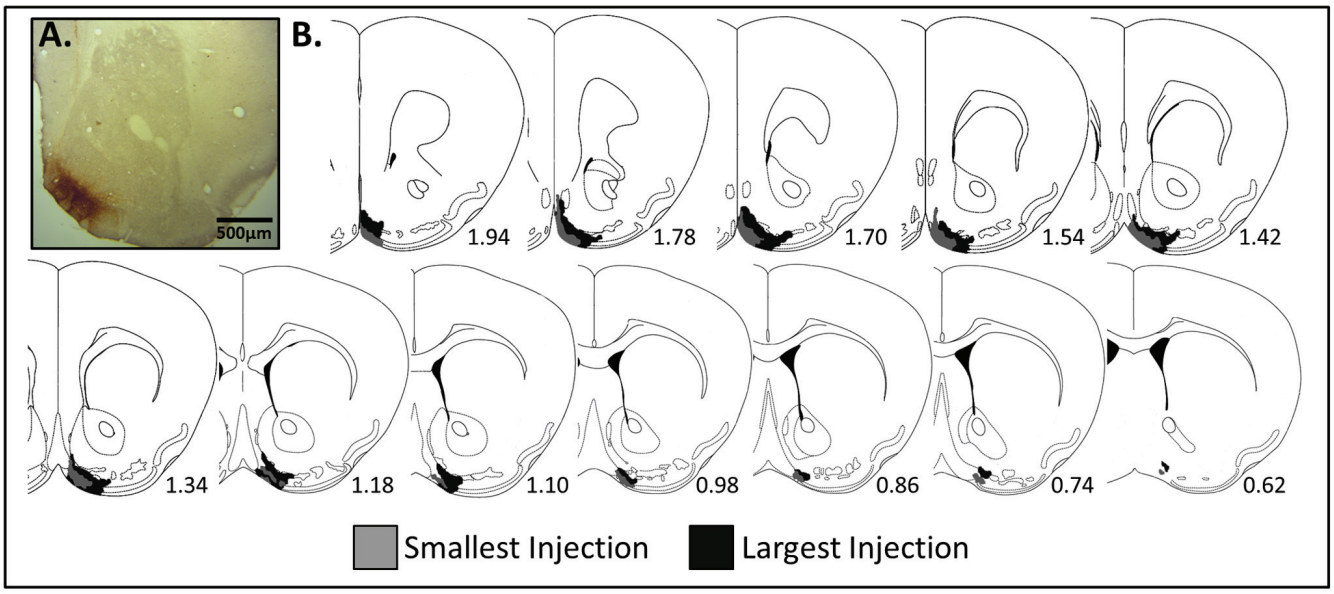

C.

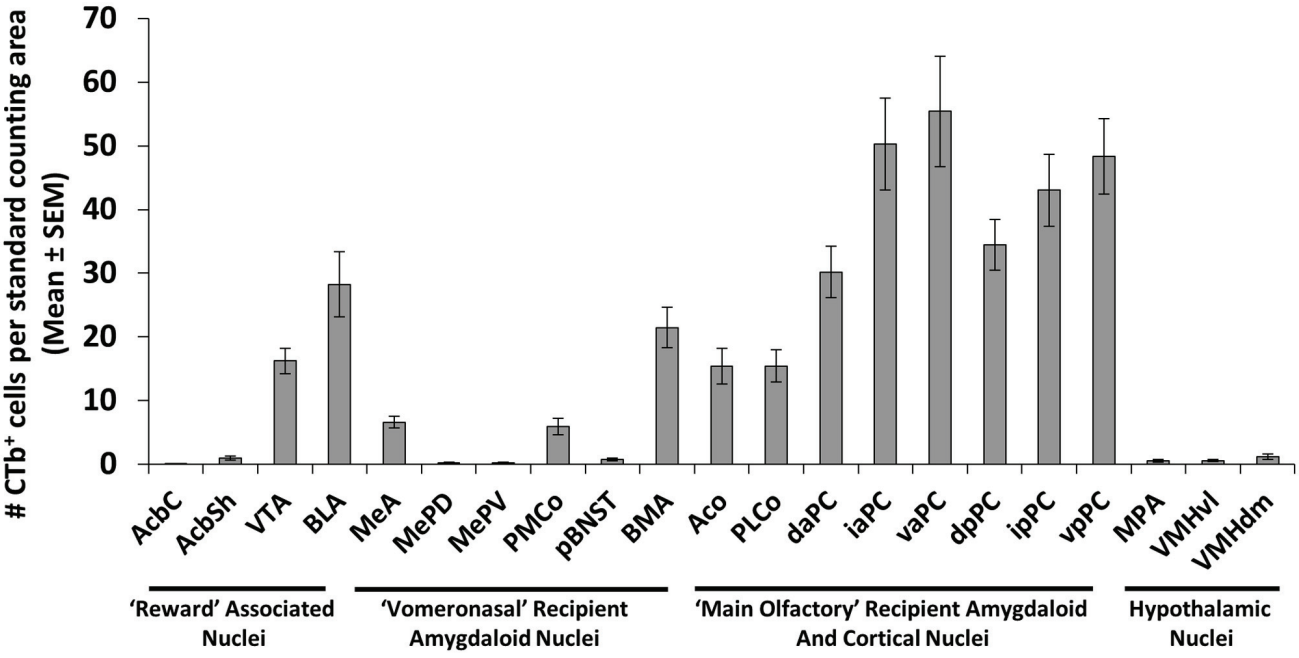

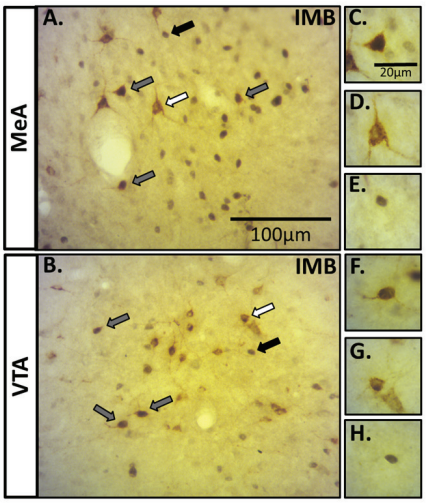

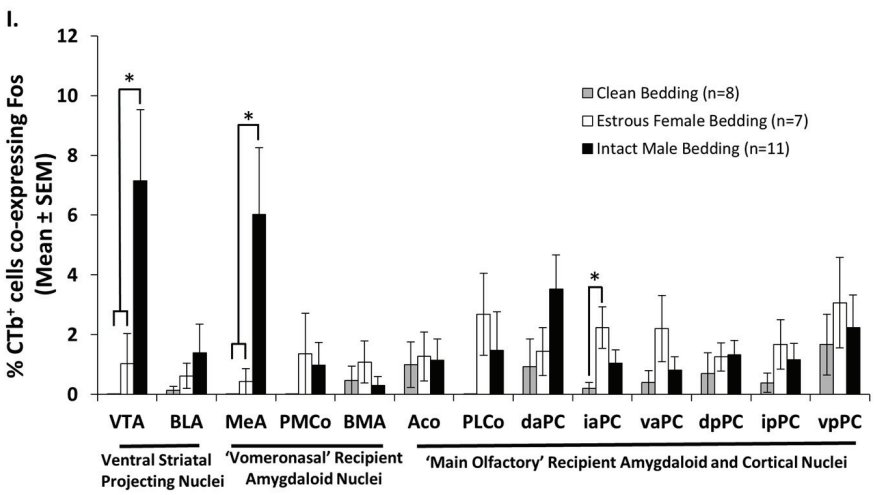

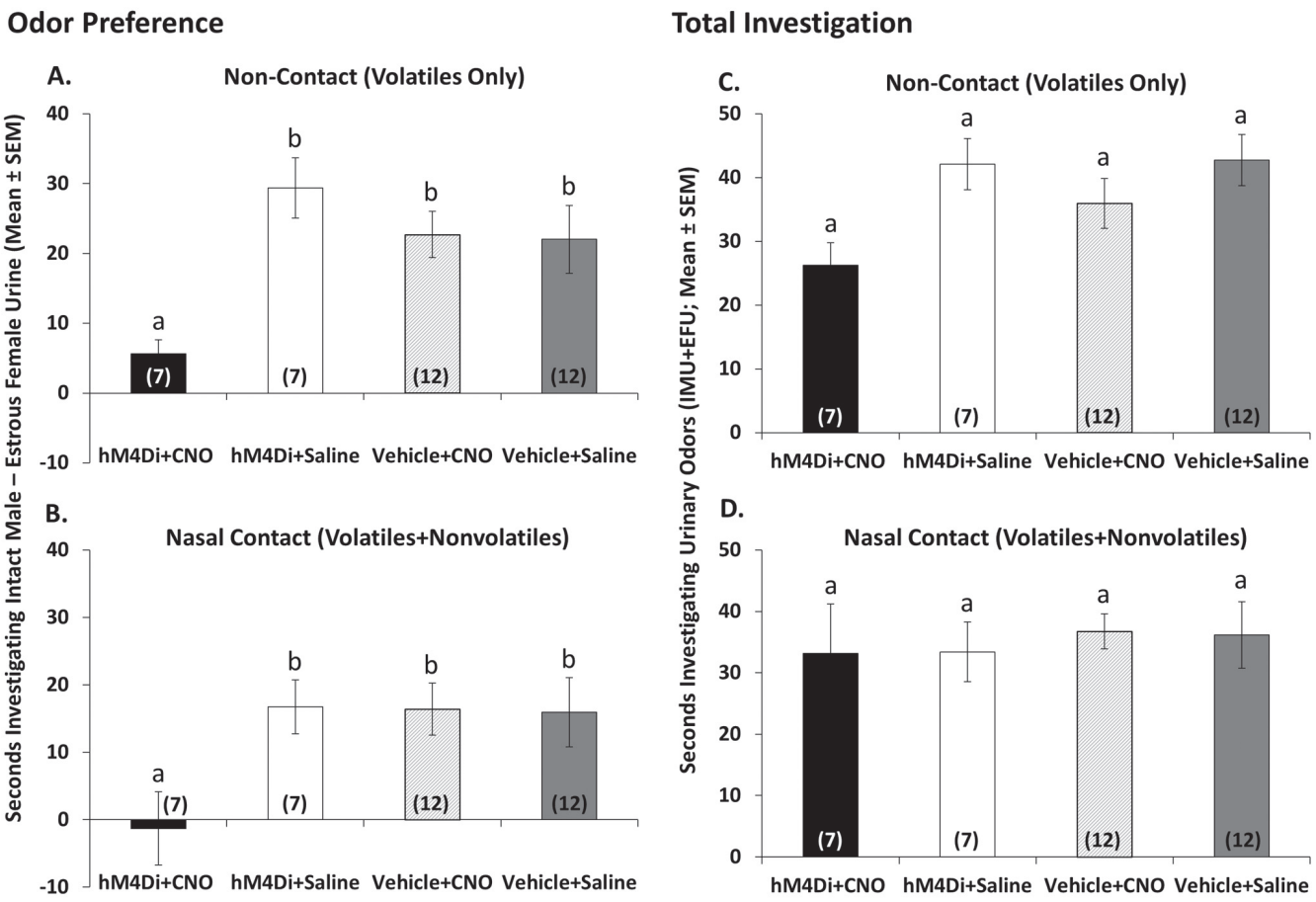

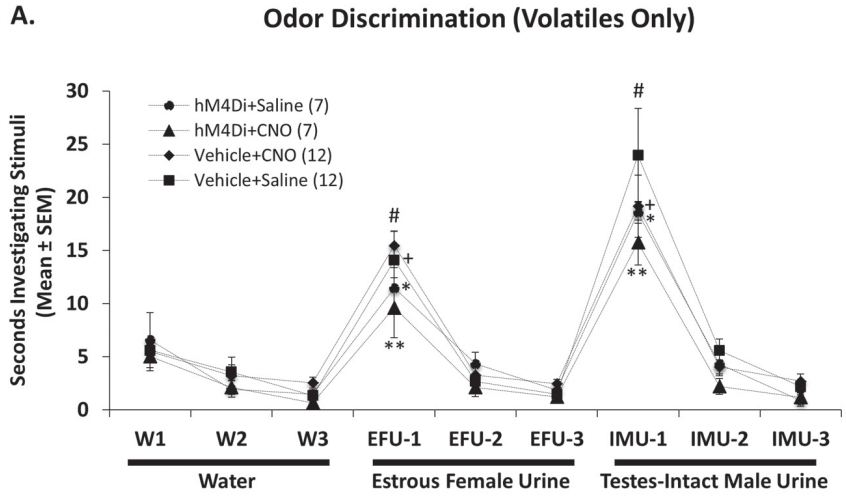

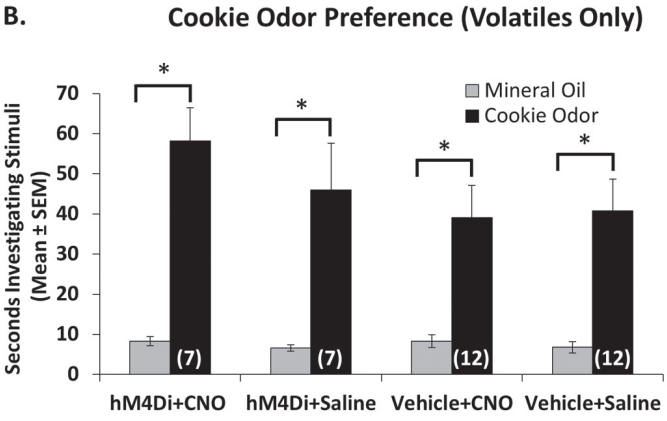

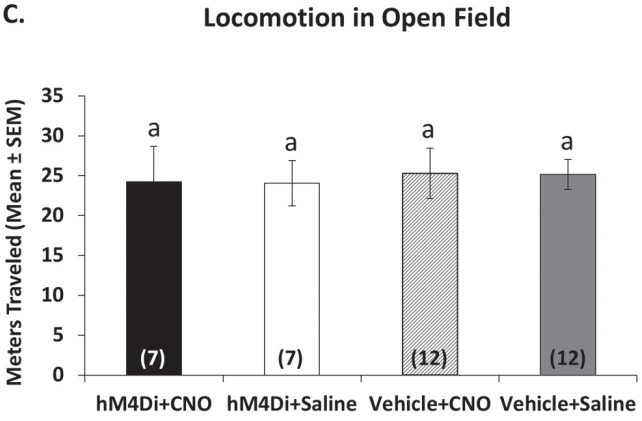

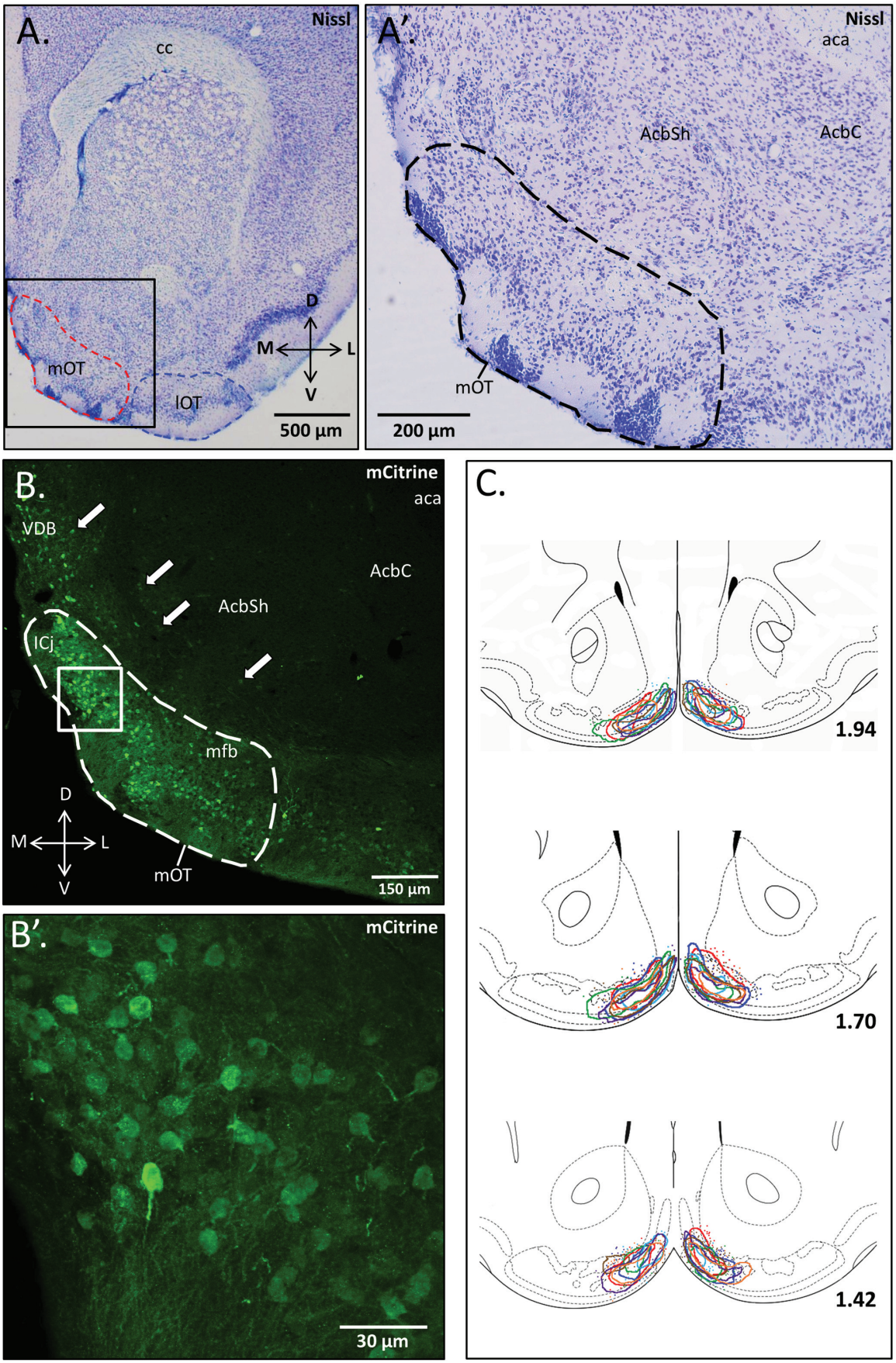

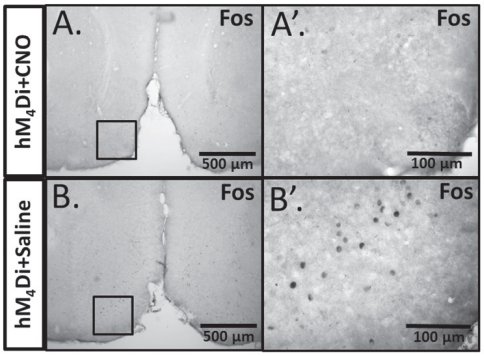

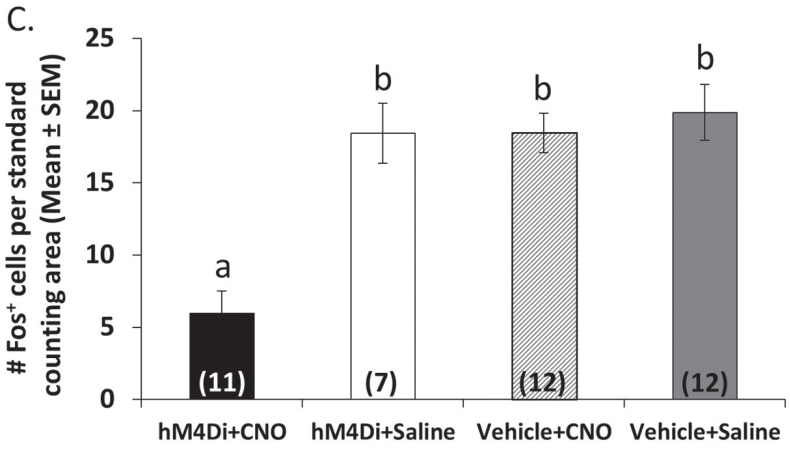

Table 1: Effect of different volatile odor stimuli (soiled bedding/urine) on forebrain Fos expression in estrous female mice

	Volatile odor stimuli			
Brain Region (no. subjects)	Clean bedding (n = 8)	Estrous female bedding/urine (n = 8)	Intact male bedding/urine (n = 11)	$F_{2,27}$ (P-value)
'Reward' associated nuclei				
AcbC	0 ± 0	0 ± 0	1 ± 0	1.6 (0.219)[c]
AcbSh*	0 ± 0	1 ± 1	11 ± 4	4.4 (0.036)[d]
VTA*	1 ± 1	3 ± 2	19 ± 6	4.9 (0.017)[e]
BLA	2 ± 1	5 ± 2	7 ± 2	1.2 (0.174)[f]
Vomeronasal recipient amygdaloid nuclei				
MeA*	2 ± 1	5 ± 2	13 ± 3	6.6 (0.005)[g]
MePD*	0 ± 0	3 ± 1	10 ± 2	7.9 (0.019)[h]
MePV*	1 ± 1	2 ± 1	11 ± 3	5.9 (0.025)[i]
PMCo*	1 ± 1	4 ± 1	9 ± 2	6.6 (0.024)[j]
pBNST	1 ± 0	2 ± 1	1 ± 1	1.1 (0.301)[k]
BMA	1 ± 1	5 ± 2	5 ± 2	1.8 (0.205)[l]
Main olfactory recipient amygdaloid and cortical nuclei				
Aco†	1 ± 0	10 ± 4	13 ± 3	4.4 (0.036)[m]
PLCo†	0 ± 0	3 ± 1	6 ± 2	4.6 (0.036)[n]
daPC	3 ± 3	11 ± 4	11 ± 4	1.3 (0.275)[o]
iaPC†	2 ± 2	9 ± 4	15 ± 3	4.6 (0.036)[p]
vaPC†	2 ± 1	7 ± 3	14 ± 3	6.1 (0.025)[q]
dpPC	3 ± 2	4 ± 2	11 ± 2	3.5 (0.064)[r]
ipPC	2 ± 1	7 ± 3	10 ± 2	3.8 (0.056)[s]
vpPC*	3 ± 1	6 ± 2	14 ± 3	5.6 (0.027)[t]
Hypothalamic nuclei				
MPA	1 ± 1	8 ± 4	11 ± 3	3.0 (0.069)[u]
VMHvl	2 ± 1	4 ± 2	8 ± 4	1.2 (0.329)[v]
VMHdm	3 ± 2	6 ± 2	12 ± 3	2.4 (0.116)[w]

Data are expressed as the mean ± SEM number of Fos-IR cells per standard counting area (300 μm^2). For each brain region, * indicates that Fos-IR in response to intact male odor is significantly greater compared to the other two odor groups; † indicates that the male odor response is significantly greater than clean bedding, but odor groups do not differ from each other (Student-Newman-Keuls *post hoc* tests following a significant [P<0.05] omnibus F-test after Benjamini-Hochberg correction for multiple testing. P-values for MeA and VTA, which were areas of a priori interest, were not corrected.) AcbC, AcbSh, nucleus accumbens core, shell; VTA, ventral tegmental area; BLA, basolateral amygdala; MeA, MePD, MePV, anterior, posterodorsal and posteroventral divisions of the medial amygdala; PMCo, posteromedial cortical amygdala; pBNST, posterior bed nucleus of the stria terminalis; BMA, basomedial amygdala; Aco, anterior cortical amygdala; PLCo, posterolateral cortical

amygdala; daPC, iaPC, vaPC, dpPC, ipPC, vpPC, anterodorsal, anterointermediate, anteroventral, posterodorsal, posterointermediate, posteroventral divisions of piriform cortex; MPA, medial preoptic area; VHMvl, VMHdm, ventrolateral and dorsomedial divisions of the ventromedial hypothalamus.

Table 2: Summary of statistical analyses. Letters (left) refer to values within the Results section.

	Data Structure	*Type of Test*	*Power*
a	Normally distributed	One-way ANOVA with SNK post hoc	0.956
b	Normally distributed	One-way ANOVA with SNK post hoc	0.086
c-w*	Normally distributed	One-way ANOVA with SNK post hoc after Benjamini-Hochberg correction	*0.581 (0.062–0.900)*
x	Normally distributed	One-way ANOVA with SNK post hoc	0.583
y	Normally distributed	One-way ANOVA with SNK post hoc	0.642
	Normally distributed	Two-way RM ANOVA with SNK post hoc	
z		drug treatment	0.551
aa		drug treatment X infection type	0.612
	Normally distributed	Two-way RM ANOVA with SNK post hoc	
bb		drug treatment X infection type	0.415
	Normally distributed	Two-way RM ANOVA with SNK post hoc	
cc		drug treatment	0.738
	Normally distributed	Two-way RM ANOVA	
dd		drug treatment	0.050
ee		infection type	0.050
ff		drug treatment X infection type	0.050
	Normally distributed	Paired t-tests, 3rd water vs 1st EFU	
gg		Test Group: hM4Di+Saline	0.998
hh		Test Group: hM4Di+CNO	0.783
ii		Test Group: Vehicle+CNO	1.000
jj		Test Group: Vehicle+Saline	0.991
	Normally distributed	Paired t-tests, 3rd EFU vs 1st IMU	
kk		Test Group: hM4Di+Saline	1.000
ll		Test Group: hM4Di+CNO	1.000
mm		Test Group: Vehicle+CNO	0.999
nn		Test Group: Vehicle+Saline	0.997
	Normally distributed	Two-way RM ANOVA	
oo		drug treatment	0.050
pp		infection type	0.164
qq		drug treatment X infection type	0.052
	Normally distributed	Two-way RM ANOVA	
rr		drug treatment	0.106
ss		infection type	0.062
tt		drug treatment X infection type	0.050
	Normally distributed	Paired t-tests, cookie odor vs mineral oil	
uu		Test Group: hM4Di+Saline	0.800
vv		Test Group: hM4Di+CNO	1.000
ww		Test Group: Vehicle+CNO	0.982
xx		Test Group: Vehicle+Saline	0.988
	Normally distributed	Two-way RM ANOVA	

yy		drug treatment	0.050
zz		infection type	0.178
aaa		drug treatment X infection type	0.059
	Normally distributed	Two-way ANOVA with SNK post hoc	
bbb		drug treatment	0.972
ccc		infection type	0.973
ddd		drug treatment X infection type	0.837

* The median and range of Power calculations are shown for this series of ANOVAs